Anti-reflection coatings for submillimeter silicon lenses

Jordan D. Wheeler*[a], Brian Koopman[b], Patricio Gallardo[b], Philip R. Maloney[a], Spencer Brugger[a], German Cortes-Medellin[c], Rahul Datta[d], C. Darren Dowell[e], Jason Glenn[a], Sunil Golwala[f], Chris McKenney[e], Jeffrey J. McMahon[d], Charles D. Munson[d], Mike Niemack[b], Steven Parshley[c], Gordon Stacey[g]

[a]CASA, University of Colorado, UCB 593, Boulder, CO, USA, 80309;
[b]Department of Physics, Cornell University, Ithaca, NY, USA 14853;
[c]Center for Radiophysics & Space Research, Cornell University, Ithaca, NY, USA 14853;
[d]University of Michigan Physics Department, 450 Church St., Ann Arbor, Michigan 48109, USA;
[e]Jet Propulsion Laboratory, 4800 Oak Grove, Pasadena, CA, USA, 91109;
[f]Division of Physics, Mathematics, and Astronomy, California Institute of Technology, Pasadena, CA, USA, 91125;
[g]Department of Astronomy, Cornell University, Ithaca, NY, USA 14853;

ABSTRACT

Low-loss lenses are required for submillimeter astronomical applications, such as instrumentation for CCAT, a 25 m diameter telescope to be built at an elevation of 18,400 ft in Chile. Silicon is a leading candidate for dielectric lenses due to its low transmission loss and high index of refraction; however, the latter can lead to large reflection losses. Additionally, large diameter lenses (up to 40 cm), with substantial curvature present a challenge for fabrication of anti-reflection coatings. Three anti-reflection coatings are considered: a deposited dielectric coating of Parylene C, fine mesh structures cut with a dicing saw, and thin etched silicon layers (fabricated with deep reactive ion etching) for bonding to lenses. Modeling, laboratory measurements, and practicalities of fabrication for the three coatings are presented and compared. Measurements of the Parylene C anti-reflection coating were found to be consistent with previous studies and can be expected to result in a 6% transmission loss for each interface from 0.787 to 0.908 THz. The thin etched silicon layers and fine mesh structure anti-reflection coatings were designed and fabricated on test silicon wafers and found to have reflection losses less than 1% at each interface from 0.787 to 0.908 THz. The thin etched silicon layers are our preferred method because of high transmission efficiency while having an intrinsically faster fabrication time than fine structures cut with dicing saws, though much work remains to adapt the etched approach to curved surfaces and optics > 4" in diameter unlike the diced coatings.

Keywords: submillimeter, artificial dielectric meta-materials, anti-reflection, Facilities: CCAT, terahertz, Parylene, SWCam, silicon, lenses

1. INTRODUCTION

As submillimeter detector arrays achieve improved sensitivity and increase in size, the demand for large low-loss optics also increases. One material commonly used for millimeter optics is high-density polyethylene (HDPE). This material, being a plastic, offers the advantage of ease of machining and when coated with Zitex® can have a reflection loss of less than 1% [1]. However, HDPE has an absorption coefficient of $\alpha \sim 0.2$ cm^{-1} at 290 K for 0.85 THz[2,3,4]. CCAT[5] instrumentation will require up to 3 different lenses; the largest of which would have an average thickness of ~ 3 cm if constructed from HDPE. The planned first-light instrument, SWCam[6,7], will observe in the 350 μm atmospheric window, 0.787 to 0.908 THz, where there are significant absorption losses, up to 30%, for the largest HDPE lens. This makes silicon the leading candidate for dielectric lenses for submillimeter astronomy. High-resistivity silicon can be manufactured using the float zone process with resistivities greater than 10,000 Ω-cm. Such silicon has a dielectric absorption coefficient of $\alpha \sim 0.01$ cm^{-1} at 290 K[8]. This process can only produce silicon with diameters less than 20 cm[9] and at least one of the 3 lenses for CCAT will be greater than this size. For larger lenses high-resistivity silicon is

*Wheeler1711@gmail.com; phone:1-(314)-574-1711

Millimeter, Submillimeter, and Far-Infrared Detectors and Instrumentation for Astronomy VII, edited by Wayne S. Holland, Jonas Zmuidzinas, Proc. of SPIE Vol. 9153, 91532Z · © 2014 SPIE · CCC code: 0277-786X/14/$18 · doi: 10.1117/12.2057011

manufactured using the Czochralski process, which can achieve resistivities of order 1000 Ω-cm, corresponding to an absorption coefficient of $\alpha \sim 0.1$ cm^{-1} at 290 K, since the absorption coefficient is inversely proportional to the resistivity of the silicon. In addition to a lower absorption coefficient, silicon's large index of refraction, n = 3.4175 at room temperature[8], results in the required lenses being over a factor of two thinner than corresponding HDPE lenses, thus reducing the path length for absorption in the lenses. An additional benefit of silicon is its high thermal conductivity, k ~ 200 Wm^{-1}K^{-1} [10], making it a great choice for cryogenic applications. The disadvantage of silicon optics is that the large index of refraction of silicon results in a 30% reflectance loss at each optical interface.

For silicon optics to provide an advantage over HDPE optics, a low loss anti-reflection coating is needed. To achieve a perfect anti-reflection coating a dielectric is needed that has an index of refraction that is the geometric mean of both materials composing an interface, $n_{coating} = \sqrt{n_1 n_2}$. For silicon lenses with indices of refraction of 3.42 making interfaces with free-space index 1, the required index of refraction is n = 1.85. Such a dielectric material with sufficiently low-loss is not readily available at submillimeter wavelengths. This study examines three options for anti-reflection coatings on silicon optics: a deposited dielectric coating, fine mesh structures cut with a dicing saw, and thin etched silicon layers, fabricated with deep reactive ion etching (DRIE), for bonding to lenses.

The first is a vapor-deposited dielectric coating of Parylene C. Deposited dielectric coatings of Parylene are commercially available, making it the easiest of the three anti-reflection coatings to manufacture. One of the downsides of using a Parylene coated lens is that the index of refraction of Parylene is n = 1.62[11] rather than 1.85. The non-optimal index of refraction of Parylene results in a reflection of 2% from 0.787 to 0.908 THz at each interface. In addition to this, Parylene has been found to have a dielectric absorption coefficient of 5.5 cm^{-1} at 0.85 THz[11]. This coefficient for a 54 μm thick 0.85 THz Parylene anti-reflection coating corresponds to an absorption loss of 3% for each interface. Parylene coatings have been previously used to create silicon optics with both sides anti-reflection coated to operate at 2 THz obtaining ~89% transmission[11].

The other two options are both examples of artificial dielectric meta-materials. The idea of artificial dielectric meta-materials exploits our ability to create structures, i.e. grooves or holes (Figure 1), in the surface of the silicon that are smaller than the wavelength of light being observed by telescopes. When the structures are sufficiently small they form a layer that interacts with light as a homogenous dielectric. Because this layer is a combination of both silicon and free space, it has an effective refractive index that lies between that of the two. The filling factor of the silicon structures can be fine-tuned so that the layer has an effective refractive index that is the ideal value of 1.85. This ability to fine-tune the refractive index to any index desired, along with silicon's low-loss, make this technique capable of producing an almost perfect anti-reflection coating. This makes anti-reflection coating using artificial dielectric meta-materials highly preferred over coating with Parylene. However, creating the sub-wavelength structures over a large diameter curved lens is more difficult than applying a vapor-deposited dielectric coating. Two methods of producing such structures are explored: making cross-cutting grooves with a silicon-dicing saw, and etching square holes using DRIE. The dicing saw technique has been demonstrated with cross-cutting dicing saw grooves to produce double layer anti-reflection coatings from 125 to 165 GHz on lenses as large as 33.4 cm in diameter with reflections reduced to tenths of a percent[9]. The DRIE method has been applied on a flat window, using grooves rather than holes, to produce 2.1 THz anti-reflection coatings with greater than 96% transmission through two interfaces[12]. This study builds upon previous research by designing and testing these anti-reflection coatings at 0.85 THz.

2. DESIGN AND MODELING OF ANTI-REFLECTION COATINGS

For a deposited dielectric coating the design and modeling is simple. The design is a quarter wavelength thick layer of dielectric material. A quarter wavelength coating with an index of refraction of 1.62 designed for 0.85 THz corresponds to a desired thickness of 54 μm. The modeling of the Parylene coated silicon as well as non anti-reflection coated silicon was performed using a transmission matrix calculation. When designing anti-reflection coatings using artificial dielectric meta-materials there are many more considerations. The pitch p, the distance between repeating structures (Figure 1), must be small enough such that $p < \lambda/(n_s + n_i \sin\theta_i)$, where n_s is the refractive index of the silicon, n_i is the refractive index of free space, θ_i is the maximum angle of incident radiation, and λ is the wavelength of incident radiation[9]. When this condition is met it ensures an anti-reflection layer will not act as a diffraction grating. When designing structures to be made with the dicing saw, a large pitch is desired. A larger pitch requires fewer cuts per interface and thus minimizes the necessary fabrication time. In this case for the DRIE single layer design, a large pitch is also desired to maximize the

width of the walls surrounding the holes so that potential non-ideality in the fabrication process, such as sloping of the walls, is small compared to the structures themselves. The initial designs for the anti-reflection structures are estimated using analytical models[13], which yield an effective refractive index given the geometry and index of refraction of the structures. For the dicing saw structures, an additional restriction is imposed: the chosen parameters must be compatible with blade widths that are commercially available. Because the size of the structures in this large-pitch limit is a significant fraction of the incident radiation's wavelength, the actual effective refractive index varies from the analytical models[9]. Thus, the analytical parameters are then varied to maximize transmission as calculated by numerical software. Both ANSYS's High Frequency Structure Simulator (HFSS) and CST Microwave Studio were used to model and optimize the transmission of the structures. The output of HFSS and CST's Microwave Studio were found to be nearly identical for the given input parameters. The design parameters of each sample tested can be found in Table 1.

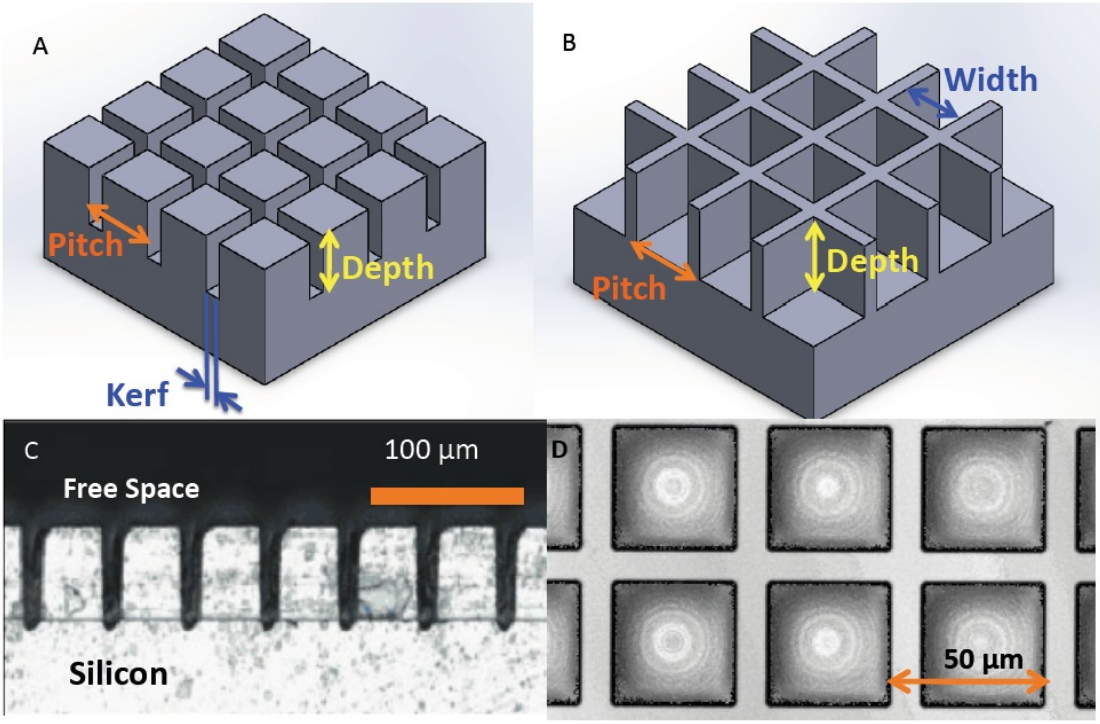

Figure 1. A. 3D model of dicing saw structures. B. 3D model of DRIE structures. C. Optical microscope picture of a cross section of grooves in dicing saw sample. This shows that the bottoms of the groves are rounded. The horizontal line at the bottom of the grooves is a result of how the wafer was cut to make this cross section. D. Overhead optical microscope picture of DRIE square holes.

Anti-Reflection Samples

	Single-Sided Dicing Saw		Single-Sided DRIE		Double-Sided Parylene	
	Design	Measured	Design	Measured	Design	Measured
Depth/Thickness	47 µm	46.5 µm	48.5 µm	48.3 µm	48 µm	45 µm
Kerf/Hole Width	13 µm	13 µm	39.3 µm	40.6 µm	N/A	
Pitch	57 µm	57 µm	50 µm	50 µm	N/A	

Table 1. Samples tested in this study.

3. FABRICATION OF ANTI-REFLECTION COATINGS

3.1 Parylene

Parylene is the common name for a variety of poly-para-xylylenes. While there are many variants of Parylene, manufacturers typically provide three types of Parylene coatings: type C, type D, and type N. Parylene C is the most common Parylene coating, popular due to its low gas and moisture permeability, and is the type tested in this study. Parylene D is a high temperature rated variant and Parylene N is known for having a larger dielectric strength while also being able to penetrate into smaller structures[14]. Parylene C and D have been found to have a refractive index of 1.62 and absorption coefficients of 5.5 cm^{-1} and 3.5 cm^{-1} respectively at 0.85 THz[11]. Parylene N has also been tested and found to have an index of refraction of 1.63 and an absorption coefficient of 3 cm^{-1} at 0.85 THz[15]. Parylene coatings are applied to a surface via vapor deposition polymerization. A crystalline dimer, i.e. powder, is first sublimated and then pyrolised. Pyrolised vapor is fed into a vacuum chamber held at room temperature, which contains the sample to be coated. Once inside the vacuum chamber vapor condenses on the substrate. The process is reported to be completely conformal, meaning that all surfaces are coated equally and conform to the sample's topology. Thickness of a coating is controlled by the amount of dimer that is used and the time the sample is left in the vacuum chamber. Typical thickness tolerances that are achieved are within 5% of the target thickness[14]. For a 54 μm target coating thickness, this amounts to an achieved thickness between 51.3 and 56.7 μm. A coating that is 51.3 or 56.7 μm instead of 54 μm results in an additional reflection loss of less than 0.25% at each interface in the frequency range from 0.787 to 0.908 THz. In theory, this process should provide an even coating over large 30 cm diameter lenses. However, this study only tested a small ~1 $inch^2$ sample and cannot currently attest to the validity of even coating over large surfaces. A 525 μm thick high resistivity silicon wafer was coated with Parylene C by Specialty Coating Systems (http://scscoatings.com/), who reported an achieved thickness of 44.4 μm for the target coating thickness of 48 μm.

3.2 Dicing Saw

Crosscutting grooves were cut into a 1x1 inch high resistivity, >1000 Ω-cm, silicon wafer with dicing blades on a three-axis CNC. For ease of fabrication, only one side of the wafer was coated. The blades utilized are specified to have a kerf, blade width (Figure 1A), between 10 and 15 μm. These are the thinnest commercially available blades. Test cuts, with several different blades, showed that the blades produced grooves with kerfs of 13 μm. Groove kerfs and depths of the final sample were measured using both an optical microscope and an optical profilometer (Table 1), both of which made measurements accurate to the nearest micron. The measurements show that the grooves are close to rectangular but exhibit curved bottoms (Figure 1C).

Recent design work has shown that anti-reflection coatings can be made the with even greater kerf, ~23 μm, blades and an 81.5 μm pitch while still maintaining the same anti-reflection efficiencies over the 0.787 THz to 0.908 THz band. This choice minimizes the number of cuts and reduces the occurrence of blade wear. 18 μm blades were tested by cutting grooves in a wafer at 1 inch s^{-1} for one hour. During this test there was not any blade breakage or difficulties while cutting. The kerf of the groove did show some evolution, on the order of 1 μm, however this is close to the detection threshold of our metrology and should be considered an upper limit. Blade cutting evolution can be mitigated by periodically dressing the saw in a ceramic block and swapping blades every 3 to 4 hours[9].

The other concern with the dicing saw method is the time required to fabricate an anti-reflection coating. The total fabrication time for the 81.5 μm pitch design on the largest of the lenses for SWCam, 30 cm diameter, at a cutting speed of 2 inch s^{-1} requires ~9 hours to coat one side. SWCam will have 7 sets of 3 lenses. The other two lenses in a set will be ~13 cm and ~20 cm in diameter. This results in a total cutting time of ~220 hours or 9 continuous days of machining. If blades are switched every 4 hours, a total of 55 blades are required. The blade manufacturers, DISCO, report safe cutting at speeds as high as 4 inch s^{-1}, which would lead to a reduction in total cutting time to ~110 hours, but speeds higher than 2 inch s^{-1} have not yet been tested for our application and should still require the same number of total blades.

While the 1x1 inch test sample was easily fabricated on a commercial 3-axis dicing saw, fabricating an anti-reflection coating on a large curved lens requires a specialized setup; this is because typical industry dicing applications only involve dicing on flat surfaces. Even though this is the case, some commercially available dicing saws may be suitable for this application, for example Advanced Dicing Technologies' (ADT) 7100 XLA, which has an 18x24 inch cutting area and 2 μm z-axis accuracy. A custom 3-axis CNC for making anti-reflection coatings at 145 GHz has been built and successfully utilized at the University of Michigan[9] accommodating lenses larger than 33 cm in diameter that is capable

of the precision necessary for the 0.787 THz to 0.908 THz band. Fabricating anti-reflection coatings at this bandpass may require a custom dicing saw facility.

3.3 DRIE

The Inductively Coupled Plasma Deep Reactive Ion Etch (DRIE, also known as Bosch) process uses high-density plasma combined with a cycle of deposition and etching to create high aspect ratio features on silicon. SF_6 is used in the etching cycle and C_4F_8 is used in the deposition cycle. The deposition cycle is used to protect the sidewalls from being etched by the SF_6 chemical etch[16,17,18,19]. The Unaxis 770 Deep Si Etcher at the Cornell Nanoscale Facility that was used to fabricate the DRIE sample is optimized for high aspect ratio deep etching. It can achieve etch rates of 2 μm per minute and 20:1 aspect ratios. Each loop of the Bosch process etches between roughly 0.3 and 0.45 μm.

A Zygo optical profiler (NewView 7300) was used to characterize the etching process. The optical profiler is used to measure the etching depth, which is then used to estimate the etching speed in each fabrication run. We have determined that etching speeds depend on the substrate quality, etching pattern and aspect ratio.

Flat 4 inch diameter wafers are patterned (Figure 2) with a 3 μm thick mask layer of photoresist using a manual spinner and a contact aligner. After development, the samples are etched using the Unaxis 770 etcher. The Bosch process has an aspect ratio that is dependent on etch rate. To obtain accurate depths, we divide the etching process into three segments. At the end of each segment, we measure the etch depth and estimate the etch speed for the next segment. Using the etch speed the required loop count is then calculated to achieve the target depth. After the Bosch process is complete, the samples are immersed in a hot solvent bath to remove photoresist.

The contact aligner can achieve a resolution of 0.8 μm. By doing lithography experiments, we were able to optimize the mask dimensions and achieve better than 1.5 μm feature size control with a 50 μm pitch pattern. This can be improved further by optimizing the mask dimensions. The vertical etch depth is found to be consistent to within 0.8 μm rms over one square inch. For a target etch depth of 48.5 μm, an average depth of 48.3 μm over one square inch was achieved. Etched surfaces were measured using the Zygo profiler. We found that there is a finite curvature on the bottom of each well, which can be described by a second-degree polynomial with an average maximum depth of 50.6 ± 0.8 μm and a radius of curvature of 93 ± 6 μm. Figure 1D shows a typical optical image of the etched features and Figure 3 shows a typical depth map.

Fabrication of DRIE patterns in a large curved surface is not a trivial task since, by design, the Bosch process provides ion impingement perpendicular to the substrate surface and chamber sizes are usually small. There are two approaches that could be used to create DRIE structures in curved-surfaces: using a custom designed and sized etcher or etching patterns on a flat surface and then plastically deforming the flat substrate into a curved shape to be bonded[20,21]. Thus far 1x1 inch samples of a one-sided single layer anti-reflection coating have been produced. We are currently scaling the process to fabricate uniform samples up to 4 inches in diameter with AR coatings on both sides.

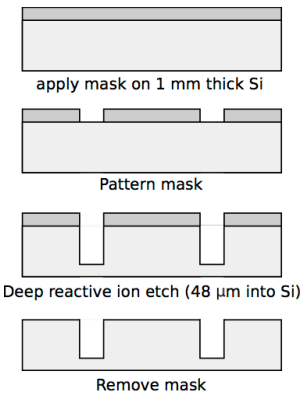

Figure 2. Fabrication Process (In order from top to bottom): Photoresist application, Mask patterning, DRIE process, Mask elimination

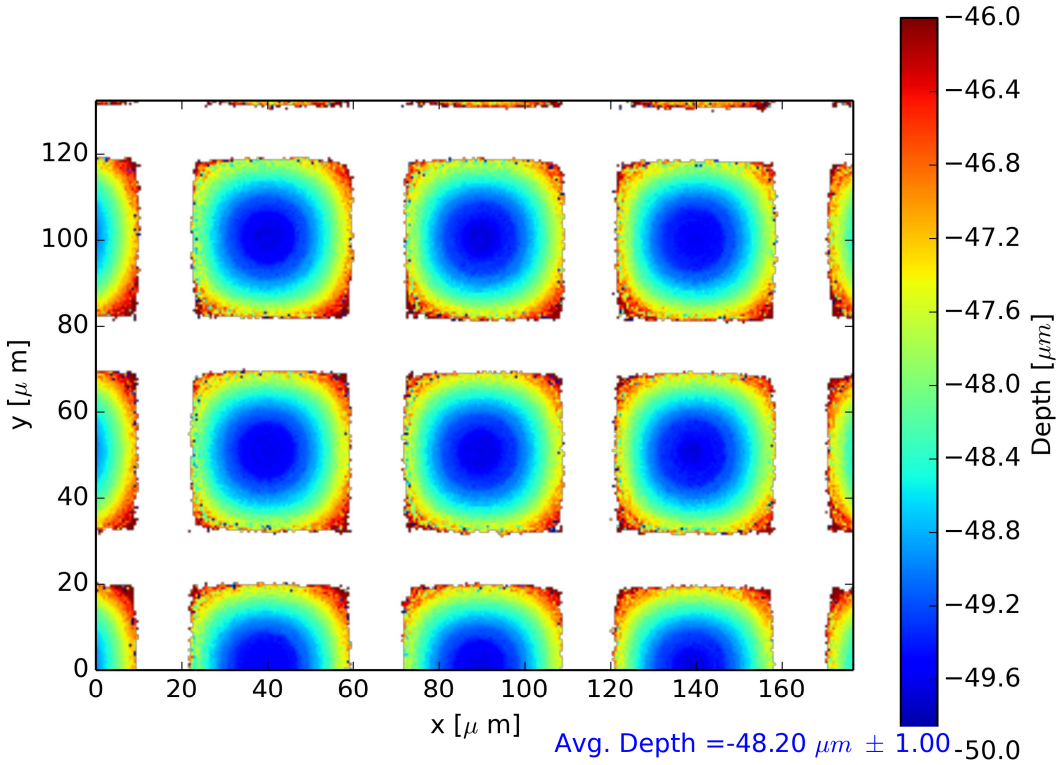

Figure 3. Trench depth map for a typical region on a DRIE sample.

4. LABORATORY MEASUREMENTS

We have developed a system that is capable of making absolute transmission measurements of 1x1 inch anti-reflection coated silicon wafers with 1% accuracy. The samples were mounted directly in front of a chopped blackbody source with a cavity temperature set to 388° C. This location was chosen to maximize the amount of radiation transmitted through the sample, hence increasing our S/N, and to avoid setting up additional resonating cavities between the sample and cryostat window. The optical path in which the samples are located has an f/# of 2.5. An f/# of 2.5 results in a distribution of angles for the radiation propagating through the silicon from 0 to 3.3 degrees, meaning that the light is nearly collimated inside our samples. Yet, modeling transmission spectrum data with a combination of normal and non-normal incident radiation does not show a significant reduction in reduced chi squared values over models containing only normal incidence radiation. After propagating through the sample, radiation then passes through a Fourier Transform Spectrometer (FTS). The FTS moveable mirror is scanned over a distance of ~20 cm, resulting in a spectral resolution of 700 MHz. Upon exiting the FTS, radiation travels into a cryostat, which contains a bolometer, coupled to the radiation via a feedhorn. The entire optical path is contained within dry nitrogen gas to mitigate the effects that humidity variation has on transmission measurements. The combination of the feedhorn cutoff frequency and metal mesh filtering yields a bandpass from 0.5 THz to 1.3 THz. When measuring over this frequency range, non-linearity in the bolometer resulted in apparent transmission measurements that were 1.2% too great (Figures 4 and 5). This was significantly reduced by using a bandpass filter to cut down the optical power incident on the bolometer, which resulted in a measurement range from 0.78 THz to 0.9 THz (Figure 6). The larger bandpass data, although non-linear, was included in the analysis because thin silicon samples act as Fabry-Perot cavities, exhibiting strong fringing (Figure 4), and the inclusion of multiple fringes better constrains model fits. Silicon without an anti-reflection coating, of which the expected transmission is well known, were measured between anti-reflection coated samples to confirm that the sample measurements are accurate (Figure 4). Such transmission measurements were found to be within 1% of the predicted transmission, suggesting that the data are also accurate to within a percent.

Transmission measurements on non anti-reflection coated 1 mm and 2 mm thick, >1000 Ω-cm resistivity, silicon samples were made to quantify absorption within the silicon. A difference of 0.44% between the two samples' transmission measurements was found; however, this is not a significant difference given that our transmission measurement confidence is only 1%. Because a difference of greater than 1% was not detected, absorption in the >1000 Ω-cm silicon should be less than 2% for the 2mm thick dicing saw sample and less than 1% for the 1 mm thick DRIE sample. The Parylene coated sample is believed to have a resistivity of 10,000 Ω-cm. For this resistivity, along with the sample thickness of 525 μm, the absorption in the silicon should be much less than a percent, but we were unable to definitively confirm the resistivity of this sample and thus absorption in the silicon cannot be entirely ruled out. If the resistivity of the Parylene sample had a value of <500 Ω-cm then absorption in the silicon could significantly affect the results.

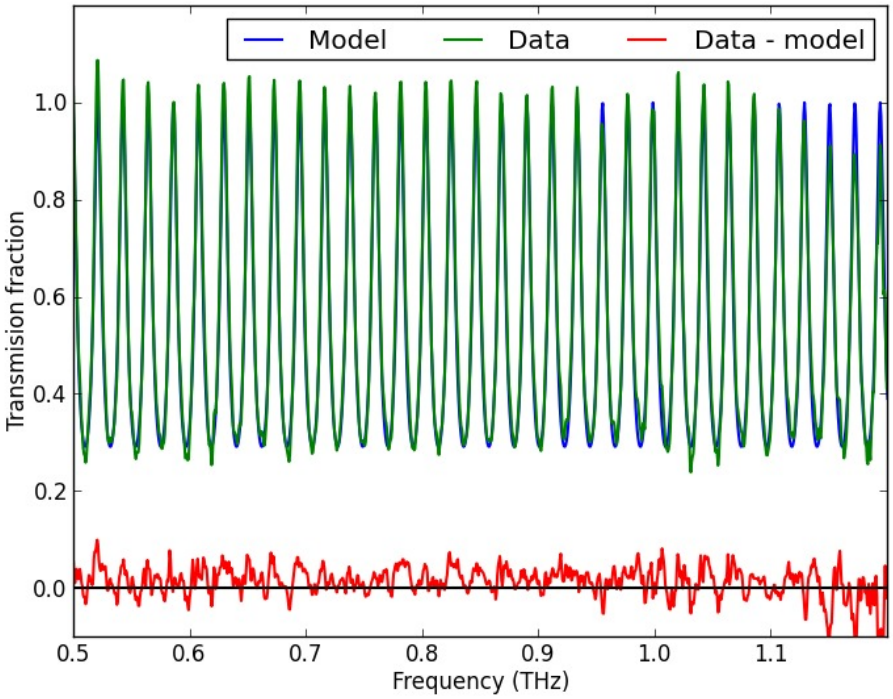

Figure 4. The measured (green) and analytically modeled (blue) transmission spectrum of a 2mm thick non anti-reflection coated silicon wafer. The red line shows the residual of the model and data. Fringing is present because the silicon wafer acts as a Fabry-Perot cavity. It was found that when using the measurement range of 0.5 to 1.3 THz, the measured transmission was systematically too great by ~1.2% due to the non-linear response of the bolometer under different loading conditions and a required normalization of the spectra to correct for the system's spectral response.

5. RESULTS

5.1 Parylene

The transmission spectra were modeled for the large measurement bandwidth, 0.5 to 1.3 THz, and for the restricted bandwidth measurement, 0.78 to 0.9 THz. The width of the silicon wafer, the thickness of the anti-reflection coatings, the index of refraction of the coatings, and the slope and intercept of an absorption coefficient assumed to vary linearly with frequency, were all allowed to vary. For the large measurement bandwidth, a best-fit width for the silicon wafer of 521 μm was found. Specialty Coating Systems reported a coating thickness of 44.4 μm, which is close to the best-fit coating thickness of 44.2 μm. A best-fit index of refraction for the Parylene was found to be n = 1.635. A best-fit absorption coefficient that varies linearly with frequency from 1.3 cm^{-1} at 0.5 THz to 13 cm^{-1} at 1.3 THz was found, but this particular variable is not considered accurate due to the non-linearity in the large bandpass measurement. Coating thickness, silicon sample thickness, and Parylene index of refraction are better constrained with large bandpass data because there are more fringes and these parameters strongly effect the location of fringe maxima and minima in frequency space. For this reason, when modeling the restricted bandpass spectrum the coating thickness, silicon

thickness, and Parylene index of refraction are the larger bandpass best-fit values. The restricted bandpass makes a linear fit to the absorption coefficient unrealistic; thus, a constant absorption coefficient was fit and the α best-fit was found to be 7.5 cm^{-1}. The 1% confidence in the measured transmission corresponds to +/- 1.2 cm^{-1} confidence in the absorption coefficient. 7.5 +/- 1.2 cm^{-1} is consistent with the value of 5.5 +/- 1.1 cm^{-1} found in previous studies[11]. Variation in the Parylene dimer could lead to an absorption that is different from that found in previous studies. The absorption coefficient of 7.5 cm^{-1}, along with the non-ideal refractive index of Parylene, results in a total transmission loss of 6% per interface (Figure 7).

5.2 Dicing Saw

Transmission measurement data, while showing the same general trends as the design models, contained noticeable differences. This is because the exact characteristics of the models are extremely sensitive to the physical dimensions of the trenches. Such sensitivity allows investigation of the original designs and the fabrication performance of these designs to a higher accuracy than can be accomplished by other optical measurements and thus provides an increased ability to optimize future designs to account for the behavior of the fabrication processes. HFSS and CST Microwave Studio are able to recreate the observed transmission spectra well, but are very time consuming on the order of hours to complete one simulation for a specific set of parameters. Due to time limitations we are not able to allow the parameters to vary freely over parameter space and thus are only able to produce simulations reasonably close to the data. The original model's parameters were varied within the measurement uncertainties of the structures and a suitable fit was found. This model, as well as transmission data, is shown in Figures 5 and 6, and model parameters can be found in Table 2. The newly derived model parameters were applied to an infinitely thick silicon model which yielded an expected a transmission for a single interface of 99.7% from 0.787 to 0.908 THz (Figure 7).

5.3 DRIE

As with the dicing saw data, the original model's parameters were varied within the measurement uncertainties of the structures and a suitable fit was found. This model, as well as transmission data, is shown in Figures 5 and 6. Model parameters can be found in Table 2. The newly derived model parameters were applied to an infinitely thick silicon model yielding an expected transmission for a single interface of 99.8% from 0.787 to 0.908 THz (Figure 7).

Anti-Reflection Modeling

	Single-Sided Dicing Saw		Single-Sided DRIE		Double-Sided Parylene	
	Measured	Model Fit	Measured	Model Fit	Measured	Model Best-Fit
Depth/Thickness	46.5 μm	47 μm	48.3 μm	47.7 μm	44.4 μm	44.2 μm
Kerf/Hole Width	13 μm	12.5 μm	40.6 μm	40.75 μm	N/A	
Pitch	57 μm	57 μm	50 μm	50 μm	N/A	
Silicon Thicknes	2 mm	2.009 mm	1 mm	1.002 mm	0.525 mm	0.521 mm
Coating Index	N/A		N/A		N/A	1.635
Silicon Absorbtion	<2%	Not modeled	<1%	Not modeled	<<1%*	Not modeled
Coating α	N/A		N/A		N/A	7.5+/-1.2 cm^{-1}*

Table 2. Model fit parameters for transmission data. *We were unable to confirm the resistivity of the silicon for the Parylene sample (the suspected resistivity is 10,000 Ω-cm). If the resistivity is actually <500 Ω-cm then there could be greater than 1% absorption in the silicon of the Parylene coated sample, which would lead to an overestimate of the absorption coefficient of the Parylene. A previous study found the value of 5.5 +/- 1.1 cm^{-1} [11].

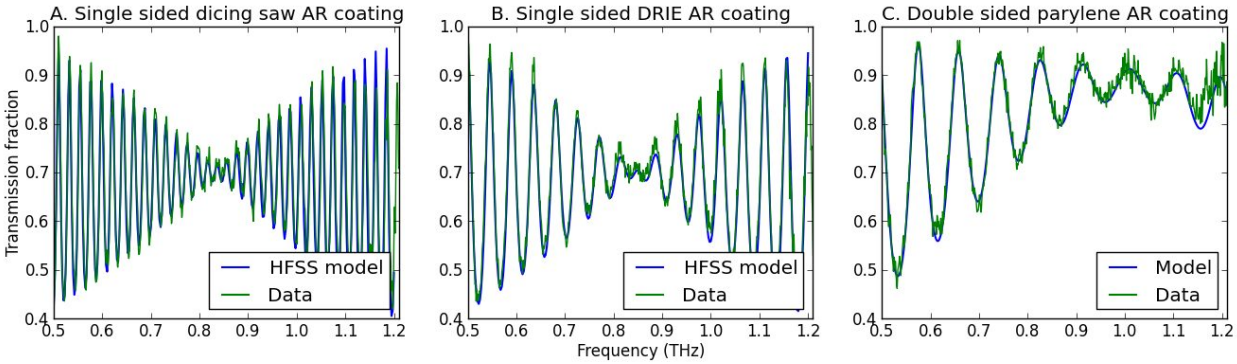

Figure 5. The measured transmissions for single-sided dicing saw structures anti-reflection coating, single-sided DRIE structures coating, and double-sided Parylene C coating. Fringing is present because the silicon wafers act as a Fabry-Perot cavity (with more fringes for thicker samples). The bowtie envelopes in A and B are caused by only one side of the silicon wafer being anti-reflection coated. This results in a minimum reflection loss of 30% due to the uncoated surface and small fringing due to the loss of one of the reflecting surfaces in the Fabry-Perot cavity. These data suffer from bolometer non-linearity and thus may be overestimating the transmission by 1.2%.

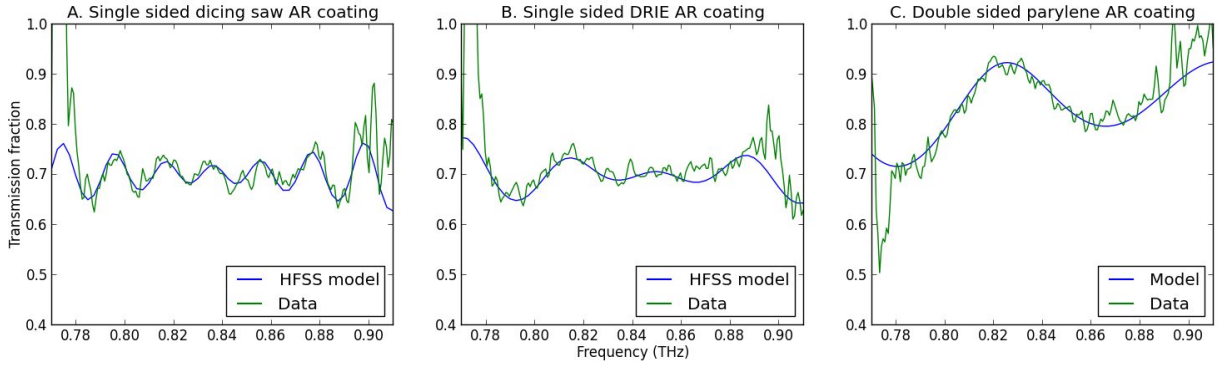

Figure 6. The measured transmissions for single-sided dicing saw structures coating, single-sided DRIE structures coating, and double-sided Parylene C coating. This data was taken with a 0.85 THz bandpass filter in the optical path and was found to not suffer from bolometer non-linearity at a level greater than 1%. The data has low S/N beyond 0.78 and 0.9 THz.

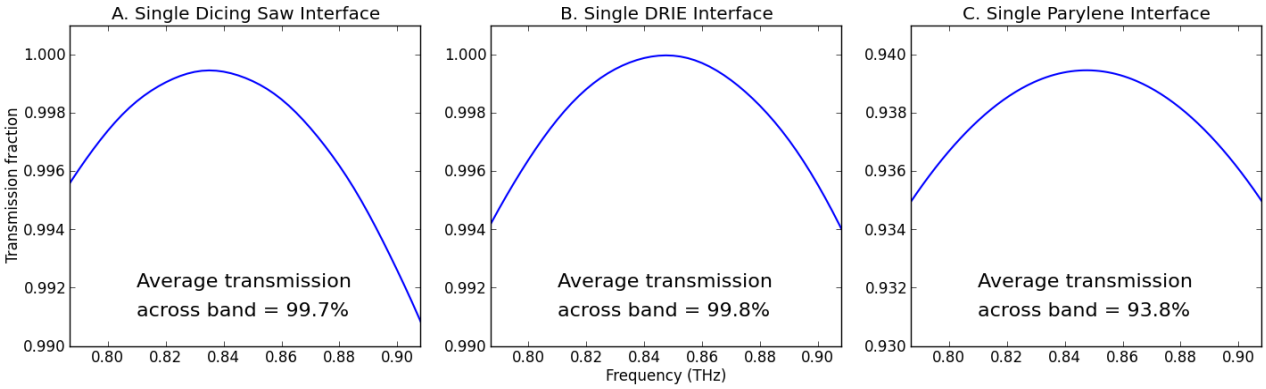

Figure 7. Model parameters found in Table 2 but applied to infinitely thick free-space and silicon slabs. The thickness of the Parylene coating has been changed to the ideal value, 54 μm, for a 0.85 THz coating. Scales of the y-axes are the same ~1%, but C is offset from A and B by 6%.

6. DISCUSSION

The relatively large transmission loss, 6%, makes Parylene C coatings the least desirable of the three methods addressed in this study. However, the ease of manufacturing a Parylene C coating provides this method with a significant advantage, making this a low risk fallback option that still exceeds the performance of traditional HDPE lenses. The Parylene anti-reflection method would benefit from additional tests on large, as well as curved, samples to quantify the uniformity of the deposition of Parylene over large areas with curvature.

Transmission efficiency (<1% loss) makes dielectric meta-material anti-reflection coatings highly preferred over Parylene anti-reflection coatings; but the intricacies of fabricating the dielectric meta-material structures make it a more complicated solution. For structures fabricated with a dicing saw, the fabrication time required can be as large as 9 hours of cutting per interface for a 30 cm diameter lens. Blade wear tests should be conducted to determine the maximum speed at which blades can be fed while still maintaining satisfactory cutting profiles and blade lifetimes. A gain of 2 times faster cutting speed would be significant. Designs should be pursued that push the boundaries of the large pitch limit, which results in decreased fabrication time. While SWCam's design and bandpass push the capabilities of the dicing saw method, it is still a realizable solution and beyond the scope of this study it may be the preferred method for small lenses or lower frequency applications.

For structures created using DRIE, the fabrication time is much smaller as a set of structures can be etched at rates of 2 μm per minute. This makes the DRIE method preferred over the dicing saw method. The process of slumping and fusing the structures to a curved lens is a new technology that still presents significant challenges to overcome. Before this method can be realized, the DRIE structures require modeling regarding how the structures will distort as they are slumped over the surface of a lens, testing of the slumping and bonding process, and testing of how these processes effect the resulting anti-reflection properties. The largest DRIE systems are currently 30 cm diameter, which limits the maximum size that can be achieved without developing a method for tiling the coatings. The DRIE method shows great promise for anti-reflection coatings at much higher frequencies where the dicing method becomes physically impossible due to lack of small enough kerf dicing blades. We plan to simulate and test samples over the range of relevant angles of incidence to confirm that they behave as predicted.

7. CONCLUSIONS

Measurements of a Parylene C anti-reflection coating at 0.85 THz were found to be consistent with previous studies and can be expected to result in a 6% transmission loss for each interface from 0.787 to 0.908 THz. Artificial dielectric meta-material anti-reflection coatings have been designed and fabricated on test silicon wafers using a silicon dicing saw and DRIE. Both were found to have reflection losses less than 1% at each interface from 0.787 to 0.908 THz. Dicing saw and DRIE structure anti-reflection coatings are very consistent with both HFSS and CST Microwave Studio simulation predictions. For CCAT we are optimistic that the DRIE coatings will realize the benefits of meta-material coatings with the lowest time and monetary costs. Thus it is the currently preferred coating option. The dicing saw coatings realize the same benefits and have been demonstrated on curved surfaces at the required precision but would require large, though practical, amounts of machining time. The dielectric vapor deposition coating of Parylene C is the least preferred method because of its low transmission efficiencies, ~6% loss per interface. However, its ease of fabrication makes a Parylene coating a low risk fallback option that still outperforms traditional HDPE submillimeter optics.

This work is supported in part by the CCAT telescope project, NSF AST-118243. This work made use of the Cornell Center for Materials Research Shared Facilities, which are supported through the NSF MRSEC program (DMR-1120296). This work was performed in part at the Cornell NanoScale Facility, a member of the National Nanotechnology Infrastructure Network, which is supported by the National Science Foundation (Grant ECCS-0335765). We are grateful to NIST-Boulder, especially Gene Hilton and Kent Irwin, for access to their dicing-saw and imaging facilities. Charles Munson is supported by NASA grant NNX12AM32H. The development of AR coatings for silicon at Michigan is supported by NASA NNX14AB58G.

REFERENCES

[1] Benford, D., Gaidis, M., and Kooi, J. "Optical Properties of Zitex in the Infrared to Submillimeter," Appl. Opt. 42, 5118-5122 (2003).

[2] Birch, J. R. and Dromey, J. D., "The optical constants of some common low-loss polymers between 4 and 40 cm^{-1}," Infrared Phys. 21, 225-228 (1981).

[3] Kawamura J., Paine S., and Papa D. C., "Spectroscopic measurements of optical elements for submillimeter receivers," Proc. of the Seventh International Symposium on Space Terahertz Technology, 349-355 (1996).

[4] Naftaly, M., Miles, R.E., Greenslade, P. J., "THz transmission in polymer materials — a data library," Infrared and Millimeter Waves, 2007 and the 2007 15th International Conference on Terahertz Electronics. IRMMW-THz. Joint 32nd International Conference on, 819-820 (2007)

[5] Woody, D. P., Padin, S., Chauvin, E., et al., "The CCAT 25 m diameter submillimeter-wave telescope," Proc. SPIE, 8444 (2012).

[6] Stacey, G.J., Parshley, S., Nikola, T., et al., "SWCam: The Short Wavelength Camera for the CCAT Observatory," in [Millimeter, Submillimeter, and Far-Infrared Detectors and Instrumentation for Astronomy VII], Holland, W.S. and Zmuidzinas, J. eds., Proc. SPIE 9153, 915321 (2014).

[7] Parshley, S.C., Adams, J., Nikola, T., Stacey, G.J., "The opto-cryo-mechanical design of the short wavelength camera for the CCAT observatory," in [Millimeter, Submillimeter, and Far-Infrared Detectors and Instrumentation for Astronomy VII], Holland, W.S. and Zmuidzinas, J. eds., Proc. SPIE 9153, 915383 (2014).

[8] Dai J., Zhang J., Zhang W., and Grischkowsky D., "Terahertz time-domain spectroscopy characterization of the far-infrared absorption and index of refraction of high-resistivity, float-zone silicon," J. Opt. Soc. Am. B 21, 1379-1386 (2004)

[9] Datta R., Munson C. D., Niemack M. D., McMahon J. J., Britton J., Wollack E. J., Beall J., Devlin M. J., Fowler J., Gallardo P., Hubmayr J., Irwin K., Newburgh L., Nibarger J. P., Page L., Quijada M. A., Schmitt B. L., Staggs S. T., Thornton R., and Zhang L., "Large-aperture wide-bandwidth antireflection-coated silicon lenses for millimeter wavelengths," Appl. Opt. 52, 8747–8757 (2013).

[10] Thompson, J.C., Younglove, B.A., "Thermal conductivity of silicon at low temperatures," Journal of Physics and Chemistry of Solids 20 (1), 146-149 (1961).

[11] Gatesman, A. J.; Waldman, J.; Ji, M.; Musante, C.; Yagvesson, S., "An anti-reflection coating for silicon optics at terahertz frequencies," Microwave and Guided Wave Letters IEEE 10 (7), 264-266 (2000).

[12] Wagner-Gentner, A., Graf, U.U., Rabanus, D., Jacobs, K., "Low loss THz window," Infrared Physics & Technology 48 (3), 249-253 (2006).

[13] Biber, S., Richter, J., Martius, S., Schmidt, L.-P., "Design of Artificial Dielectrics for Anti-Reflection-Coatings," Microwave Conference, 2003. 33rd European, 1115-1118 (2003)

[14] http://www.paryleneengineering.com/properties.html

[15] Lee, K.-S., Lu, T.-M., and Zhang, X.-C. "Tera Tool," IEEE Circuits & Devices Magazine, 18 (6), 23–28 (2002).

[16] Ji J., Tay F., Miao J, and Sun J. "Characterization of silicon isotropic etch by inductively coupled plasma etcher for microneedle array fabrication," Journal of Physics: Conference Series 34 (1), 1137-1142 (2006).

[17] McAuley S A, Ashraf H, Atabo L, Chambers A, Hall S, Hopkins J, and Nicholls G. "Silicon micromachining using a high-density plasma source," Journal of Physics D: Applied Physics 34 (18), 2769-2774 (2001).

[18] Larmer, F. and Schilp, A., "Method for anisotropically etching silicon," German Patent DE4241045, (1992).

[19] Britton J.W., Nibarger J.P., Yoon K.W., Beall J.A., Becker D., Cho H.-M., et al. "Corrugated silicon platelet feed horn array for CMB polarimetry at 150 GHz," Proceedings of SPIE - The International Society for Optical Engineering, 7741 (2010).

[20] Nakajima K., Fujiwara K., Pan W., and Okuda H. "Shaped silicon-crystal wafers obtained by plastic deformation and their application to silicon-crystal lenses," Nature Materials 4 (1), 47-50 (2004).

[21] Tong Q.-Y., and Gösele U. [Semiconductor wafer bonding: science and technology], John Wiley, New York (1999).